HHS Public Access

Author manuscript

Hear Res. Author manuscript; available in PMC 2020 July 01.

Published in final edited form as:

Hear Res. 2019 July ; 378: 3–12. doi:10.1016/j.heares.2019.01.015.

Distortion product otoacoustic emissions: sensitive measures of tympanic -membrane perforation and healing processes in a gerbil model

Wei Dong[1,2], **Glenna Stomackin**[1], **Xiaohui Lin**[1], **Glen K Martin**[1,2], and **Timothy T Jung**[1,2]

[1]Research Service, VA Loma Linda Healthcare System, Loma Linda, CA 92357 USA

[2]Department of Otolaryngology--Head & Neck Surgery, Loma Linda University Health, Loma Linda, CA 92354 USA

Abstract

Distortion product otoacoustic emissions (DPOAEs) evoked by two pure tones carry information about the mechanisms that generate and shape them. Thus, DPOAEs hold promise for providing powerful noninvasive diagnostic details of cochlear operations, middle ear (ME) transmission, and impairments. DPOAEs are sensitive to ME function because they are influenced by ME transmission twice, i.e., by the inward-going primary tones in the forward direction and the outward traveling DPOAEs in the reverse direction. However, the effects of ME injuries on DPOAEs have not been systematically characterized. The current study focused on exploring the utility of DPOAEs for examining ME function by methodically characterizing DPOAEs and ME transmission under pathological ME conditions, specifically under conditions of tympanic-membrane (TM) perforation and spontaneous healing.

Results indicated that DPOAEs were measurable with TM perforations up to ~50%, and DPOAE reductions increased with increasing size of the TM perforation. DPOAE reductions were approximately flat across test frequencies when the TM was perforated about 10% (<1/8 of pars tensa) or less. However, with perforations greater than 10%, DPOAEs decreased further with a low-pass filter shape, with ~30 dB loss at frequencies below 10 kHz and a quick downward sloping pattern at higher frequencies. The reduction pattern of DPOAEs across frequencies was similar to but much greater than, the directly measured ME pressure gain in the forward direction, which suggested that reduction in the DPOAE was a summation of losses of ME ear transmission in both the forward and reverse directions. Following 50% TM perforations, DPOAEs recovered over a 4-week spontaneously healing interval, and these recoveries were confirmed by improvements in auditory brainstem response (ABR) thresholds. However, up to 4-week post-perforation, DPOAEs never fully recovered to the levels obtained with normal intact TM, consistent with the incomplete recovery of ABR thresholds and ME transmission, especially at

Corresponding author: Wei Dong, Research Service – 151, VA Loma Linda Healthcare System, 11201 Benton Street, Loma Linda, CA 92357 USA, Tel: 909 825 7084, Ext. 2899, Fax: 909.796.4508 wdong@llu.edu.

high-frequency regions, which could be explained by an irregularly dense and thickened healed TM.

Since TM perforations in patients are commonly caused by either trauma or infection, the present results contribute towards providing insight into understanding ME transmission under pathological conditions as well as promoting the application of DPOAEs in the evaluation and diagnosis of deficits in the ME-transmission system.

Keywords

hearing; middle ear function; distortion product otoacoustic emissions; tympanic membrane perforation; spontaneously-healed tympanic membrane; middle ear pressure gain

1. Introduction

The ear is a sensitive and selective detector of acoustic stimuli. Active processes in the ear's end organ, the cochlea, create sounds that leak back out through the middle ear (ME) to the ear canal. These sounds, measured in the ear canal by a sensitive microphone, are termed "otoacoustic emissions (OAEs) (Kemp, 1978). OAEs carry information about the mechanisms that generate and shape them and they have been used in both the laboratory and audiology clinic as a noninvasive tool to diagnose hearing impairment (Lonsbury-Martin et al., 1990; Probst et al., 1991; Shera, 2004). The ME, consisting of the tympanic membrane (TM) and three ossicles, known as the malleus, incus, and stapes, is responsible for transmitting sound in and out of the cochlea and, thus, molds the OAEs. For example, the ME shapes two-tone elicited distortion product otoacoustic emissions (DPOAEs) twice, i.e., by the inward-going primary f_1 and f_2 tones in the forward direction and the outward traveling DPOAEs in the reverse direction. Thus, any disorders of the ME would influence both the forward and reverse sound transmission, which would lead to alterations in the DPOAEs. Although the influence of the ME on OAEs has been extensively studied [see reviews by Zhao et al. (2000) and Tlumak et al. (2001)], OAEs are routinely used in the clinic in the diagnosis of sensorineural hearing loss, specifically relating to the active cochlear process known as cochlear amplification (Allen et al., 1992; de Boer et al., 2005; Dong et al., 2013; Shera et al., 2007), rather than for identifying ME impairments, which have not been systematically characterized and differentiated from patterns of sensorineural hearing loss.

Under normal conditions, ME-sound transmission in both the forward and reverse directions has been measured in cat (Voss et al., 2004), gerbil (Dong et al., 2006), and guinea pig (Magnan et al., 1997), as well as in human temporal bone specimens (Puria, 2003). ME reverse transmission has also been explored using OAEs combined with theoretical models (Dalhoff et al., 2011; Keefe, 2002; Naghibolhosseini et al., 2017; Voss et al., 2004). In gerbils, sound transmissions along the stapes piston-like motion direction from the lateral process of the malleus to the long process of the incus in the forward and reverse directions were found to be similar (Dong et al., 2012). However, the pressure loss in the reverse transmission was found to be greater than the gain in the forward direction, probably due to

the different load impedances involving the cochlea in the forward and the ear canal in the reverse transmission (Dong et al., 2006).

The uniqueness of the TM's morphology and its physical properties determine its normal pattern of vibration that is imparted to the malleus to which it attaches. TM ruptures, or perforations, alter its structural and mechanical properties, thus resulting in a deterioration of sound transmission, which presents clinically as a conductive hearing loss (CHL) (Merchant et al., 2003a). Moreover, the healed TM is thickened and abnormally dense, which also contributes to the resulting elevated hearing thresholds (Cho et al., 2013; Garth, 1994). In some cases, surgical reconstruction of the TM in the form of a tympanoplasty is performed when there is a perforation in the TM. Clinical observations indicate that the surgical techniques used to repair a perforated TM can lead to some restoration of the CHL postoperatively (Merchant et al., 2003a; Merchant et al., 2003b). However, in up to 30% of patients, there remains an abnormal residual air/bone gap that may vary from 5–35 dB (Puria et al., 2013), which continues to produce hearing difficulties.

In clinics, the condition and mobility of the TM and ossicles are normally assessed through otoscopy, tympanometry (tympanogram), and audiograms with air or bone stimulation. Otoscopy provides a visual assessment of the TM without any functional evaluation. Tympanometry is an objective test of ME function, which provides information on how admittance varies with pressure in the ear canal, and must be combined with audiograms for accurate hearing evaluation. Because the application of pressure to the ear canal may lead to further TM damage or a 2nd time TM perforation during the spontaneous healing period, it may not be the best choice for diagnosing certain TM pathological conditions. Tympanometry results also vary within the same pathological condition, making them unable to accurately pinpoint the exact ME problem (Shanks, 1984). Audiograms plot hearing thresholds versus frequency, which are the summed results along the auditory pathway up to the brain. To quantify CHL, air-bone gap measurements are ordinarily used, which demonstrate the threshold differences between air-and bone-stimulation. However, bone stimulation bypasses the ME ossicular chain and usually only goes up to 8 kHz instead of covering the whole human hearing range of 20 Hz to 20 kHz. In short, these conventional methods diagnose TM abnormalities, but do not provide a precise description across the whole hearing frequency range of ME transmissions under pathological TM conditions. Thus, there is a need to develop a simple and straightforward diagnostic tool to evaluate ME function involving pathology.

The current study focused on systematically exploring the utility of DPOAEs for characterizing ME disorders, specifically following TM perforations and the subsequent spontaneous healing process. In the present study, the effects on normal DPOAEs following altered ME function due to TM perforation and spontaneous healing were studied in a gerbil model. This approach allowed ME transmission to be explored under pathological conditions, especially after the TM had spontaneously-healed post-perforation. In particular, it allowed us to explore DPOAEs over a wide frequency range to provide pre-,during-,and post-evaluations of the status of ME function. In addition, ME pressure gain (MEPG) under these conditions was directly measured by the comparison of pressure responses in scala vestibuli (SV) next to the stapes and in the ear canal close to the TM. Study results provided

a systematic description of ME function and its effects on DPOAEs under these pathological conditions, which may provide guidelines for the clinical application of DPOAEs under various abnormal ME states.

2. Materials and methods

2.1. Experimental design

To evaluate the effects of the TM perforations and the spontaneously-healed TM perforations on both DPOAEs and sound transmission through the ME, specific experiments focused on obtaining measures of DPOAEs and ME transmission in gerbils with intact ossicular chains under two distinct pathological conditions.

2.1.1 Mechanically-induced TM (pars tensa) perforations ranging from miniscule to its complete removal—To quantify TM perforation effects on DPOAEs and ME transmission, pressure responses at the TM (P_{TM}) and in the SV (P_{SV}) to single or 2-tone stimulation at 80 or 90 dB SPL were simultaneously measured (Fig. 1A) in the left ear *in vivo* under conditions of an intact TM followed by mechanically-induced perforations. TM perforations were progressively increased in size from the inferior aspect and extended towards the posterior direction (Fig. 1B), so that each gerbil contributed multiple data points to these measurements (Stomackin et al., 2018). The features of the induced TM perforations including size, shape, and location were documented using a Laser Doppler Vibrometer's camera system. TM perforations were made in sequence of a hole (200–400 μm in diameter, referred to as a size of <3%), <1/8 (~10%), 1/4 (25%), 1/2 (50%), 3/4 (75%) and 100%, leaving only the portion of the TM attached to the manubrium, the pars flaccida, and the ossicular chain intact (Fig. 1B). The area of the intact gerbil pars tensa has been reported as 13–17 mm^2 (Buytaert et al., 2011; Cohen et al., 1992; Mason, 2016; Ravicz et al., 1992; Teoh et al., 1997), and if we used a value of 14 mm^2 to calculate the sizes of our perforations, the corresponding areas were <0.42 (<3%), 1.4 (~10%), 3.5 (25%), 7.0 (50%), 10.5 (75%), and 14 mm^2 (100% removal). The location effects on ME transmission were similar with similar sized TM perforations (McArdle et al., 1968; Mehta et al., 2006; Pannu et al., 2011; Park et al., 2015; Stomackin et al., 2018; Voss et al., 2000; Voss et al., 2001a; Voss et al., 2001b; Voss et al., 2007) and thus are not discussed in the current report.

2.1.2 The spontaneous healing of a 50% TM perforation over 4 weeks of recovery—Each gerbil received a single 50% TM perforation at the inferior region in the left ear (Fig. 1C), which was permitted to spontaneously heal over a 4-week post perforation period. Over this time course, hearing restoration was evaluated by measuring auditory brainstem response (ABR) thresholds and DP-grams, i.e., $2f_1-f_2$ DPOAE levels as a function of f_2 frequency, at key time points, i.e., at day one before and after the TM perforation and following every week up to 4-week post-perforation. At 5-week, P_{TM} and P_{SV} were simultaneously measured and the results were compared to the results of normal intact TM obtained from group #1 described above. At the end of the experiment, the TMs from both ears of the same subject were harvested, with one ear exhibiting a spontaneously-healed TM post-perforation and the other ear serving as a control. The healed TMs were found to be thickened and denser in the perforation region compared to normal controls. A

detailed report on the thicknesses of the TMs measured using Optical Coherence Tomography (Thorlabs) is in a separate manuscript under preparation.

2.2 Animal preparation

The care and use of animals were approved by the Institutional Animal Care and Use Committee (IACUC) of the VA Loma Linda Healthcare System. Young adult Mongolian gerbils (N=44) contributed to the study, with 24 gerbils contributing to the mechanically-induced TM perforations and 20 gerbils contributing to the spontaneously-healed post-perforation experiments. For the mechanically-induced TM perforation experiment, 8/24 animals contributed to data points with a complete perforation set. The other animals were either used to develop the experimental approach or were excluded from the statistics due to incomplete data sets. For the spontaneously-healed post-perforation experiments, 6/20 animals were included in the final statistics for the spontaneously-healed MEPG measurements. The other animals were used to establish the experimental technique or were removed from the study due to ear infections or incomplete data sets.

For the MEPG measurements (Fig. 1A) under conditions of mechanically-induced TM perforations (Materials and methods 2.1.1) and spontaneously-healed TM perforations after 4-week post-perforation (Materials and methods 2.1.2 after 4-week post-perforation), each animal was deeply anesthetized with a ketamine (80 mg/kg)/xylazine (10 mg/kg) cocktail and maintenance doses (1/3 of initial dose) were given as needed. The animal's body temperature was maintained at ~37° by a rectal probe attached to a Harvard Apparatus heating pad. The animal's skull was secured to a head-holder using dental cement (Durelon), and a tracheotomy was performed to maintain a patent airway. To introduce the micro-pressure sensor, the left pinna was removed and the bulla was widely opened with great care to place a small hand-drilled hole through the bony wall of the SV, just next to the stapes (Dong and Olson, 2006; Olson, 1998). During this procedure, the cochlear condition was monitored by measuring DPOAEs at several key time points, i.e., pre-surgery, post-opening bulla, post-introducing the SV hole, and after introducing the sensor.

For the timely monitoring of hearing restoration over the post-perforation time course of TM healing (Materials and methods 2.1.2 up to 4-week post-perforation), both ABRs and DPOAEs were measured in the form of tone-burst specific thresholds and DP-grams, respectively, after the animal was anesthetized with the ketamine/xylazine cocktail. During a measurement session, maintenance anesthetic doses were given as needed as indicated by the toe-pinch method, and following each recording session over a 4-week post-perforation period, a 1-week recovery interval was permitted between each weekly recording.

2.3 Stimulus presentation, data acquisition, and analysis

To achieve the goals of experiments listed above, two different well-established data acquisition systems were used with detailed descriptions below.

2.3.1 Mechanically-induced TM perforation experiments—Single tone sweeps and two-tone stimuli (L_1=L_2 with a fixed f_2/f_1 ratio of 1.25) were generated by a commercial system [Tucker-Davis Technologies (TDT) System III] with a sampling rate of 200 kHz

driving one or two Fostex speakers. Stimulus and acquisition software was written in MATLAB and the TDT visual design studio, and responses were analyzed by fast Fourier transforms (FFT) using MATLAB.

A Y-tube sound system was coupled to the ear canal opening in an open-field sound configuration with a Sokolich ultrasound microphone's probe tube passing through the center of the sound tube, and the tip of the microphone positioned close to within ~3 mm of the TM where the sound pressure levels (SPL) of acoustic stimuli were calibrated in decibels (dB) re 20 μPa p-p. The open-field sound configuration was due to a small hole being made superior to the ear canal to access the TM to create the perforations.

The two arms of the Y-tube connected to the two Fostex speakers. The microphone also served as the receiver of the acoustic pressure at the TM (P_{TM}). With 1-s data acquisition times, the probe-tube microphone noise level was about −10 dB SPL. The system distortion level was regularly checked in a cavity corresponding to the volume of the gerbil ear canal and was at least 60 dB below the level of the primary tones when their levels were 90 dB SPL (Dong, 2017).

MEPG measurements: To directly measure the MEPG, high-level tones were used, i.e., 80 or 90 dB SPL. Pressure responses at the TM near the umbo (P_{TM}) and in the SV near the stapes (P_{SV}) were simultaneously measured using a Sokolich ultrasound probe-tube microphone and a micro-pressure sensor (see Fig. 1A). The micro-pressure sensor was described previously (Dong et al., 2008; Olson, 1998). The tip of the micro-pressure sensor has a cylindrical shape, with an outer diameter of ~120 μm (Dong et al., 2008). The micro-pressure sensor was calibrated individually both in room and body temperature in air after construction and before and after measurements. MEPG was used to characterize ME-sound transmission from the TM to the cochlea and is defined here as $MEPG=|P_{SV}/P_{TM}|$.

2.3.2 Spontaneously-healed TM perforation experiments

Hearing evaluation at key time points: DPOAE and ABR tests were performed at key time points, i.e., at day one pre-and post-50%-perforation of the pars tensa, and during a recovery period over 4 weeks. These hearing tests were done using another well-established system described in detail elsewhere (Martin et al., 2011). Briefly, tone stimuli were generated by a PC based dynamic signal analyzer board (NI PCI-4461, National Instruments, Austin, TX) using one or two Radio Shack speakers. This same board was used to measure ear canal sound pressure from an ER10B+ (Etymotic Research) microphone assembly, which was sampled at 176.4 kHz and synchronously averaged (n=4) by the DSP board. For DPOAEs, the levels of responses at stimulus frequency or distortion product frequencies and their related noise floors were extracted from a 16384-point (band width=10.77 Hz) FFT of the average time sample. For ABRs, a synchronously averaged (n=512) 2048-point time sample was taken in order to visualize ABR waveforms. For both types of measures, the sound was introduced into the ear canal via a closed-field configuration. Data acquisition was performed using custom LABVIEW software and analysis was done using MATLAB.

DP-grams: To elicit $2f_1-f_2$ DPOAEs, two equilevel ($L_1=L_2$) primary tones (30 to 75 dB SPL in 5 dB steps) at f_1 and f_2, with a fixed f_2/f_1 ratio of 1.25, were used to generate DP-grams as a function of f_2 frequency ranging from 1–40 kHz in 0.1-oct steps. The ER10B+ microphone was positioned into the ear canal in a closed-field sound configuration

ABRs: ABRs evoked by single tone bursts were recorded over the recovery time course at frequencies of 0.5, 2, 4, 5.6, 8, 11.3, 16, 22.6, 32, and 45 kHz with stimulus intensity from 0 to 80 dB SPL in 5 dB steps. Electrodes were placed in a subdermal location with the recording electrode positioned at the vertex of the skull, the reference electrode placed under the ear canal opening near the bulla location, and a ground electrode placed in the left rear leg. ABR thresholds were determined by visually examining the ABR wave I to determine the lowest sound level at which reproducible waveforms were observed.

MEPG measurements: After 4-week post-perforation, MEPG under the spontaneously-healed condition were measured in the same way as the above 2.3.1 section "MEPG measurements."

2.3.3 System distortion—For all measurements, system distortion levels were verified by recording DPOAEs induced by high-level primary tones, i.e., 90 dB SPL, under conditions of disarticulating the incus and stapes *in vivo* and/or post-mortem. The responses at all frequencies were in the noise floor, thus confirming that our measurements were not artificially due to system distortion.

2.4 Statistical analysis

Data collected from different gerbils under similar conditions, i.e., DPOAEs, ABR thresholds, magnitudes of pressure (P_{TM} and P_{SV}) and calculated quantities to describe ME transmission in the form of MEPG, were averaged at each testing frequency separately, and the mean and standard deviation (SD) for all data points were calculated using MATLAB. In addition, a Student's paired *t*-test was used to determine if the mean values of these quantities and variations under the various TM perforation conditions were statistically significant from those under the normal intact TM conditions. The Student's paired *t*-test was performed over three frequency bins, i.e., <10 kHz, 10–20 kHz, and >20 kHz for DPOAEs and <10 kHz, 10–30 kHz, and >30 kHz for other quantities such as the MEPG. For all statistics, a p-value <0.05 was considered significant, and the statistical results are presented below.

3. Results

Responses were similar across animals under the same conditions. The main findings are described below by examples from an individual gerbil followed by averaged responses across animals. Responses under normal intact TM conditions formed the baselines (gray lines in following figures) to quantitatively characterize the reduction patterns under TM pathological conditions. Illustrations depicting the results are focused on the largest commonly used $2f_1-f_2$ DPOAEs evoked by high-level primary tones, to provide variation patterns over a wide frequency region.

3.1 DPOAEs and ME sound transmission under systematically enlarged TM perforation conditions

Effects of mechanically-induced with systematically enlarged TM perforations on DPOAEs and ME sound transmissions were illustrated by responses of $2f_1-f_2$ DPOAEs and MEPG (Fig. 2), with panels A-C showing results from a representative animal (Expt. #3) and panels D and E displaying the averaged data across animals together with ±1 times SD. Under normal intact TM conditions, the $2f_1-f_2$ DPOAE evoked by equal-intensity stimulation of 90 dB SPL and an f_2/f_1 ratio of 1.25 was robust, ~40–50 dB SPL across frequencies (gray lines in Fig. 2A), consistent with results published in the literature (Dong et al., 2006; Dong et al., 2008; Dong et al., 2017). The $2f_1-f_2$ DPOAE decreased with increasing size of TM perforation and was only around 10 dB when TM perforation reached ~50% of the pars tensa (dotted blue lines in Fig. 2A). Above 25% perforation, there was more reduction of DPOAEs at higher frequencies, i.e., f_2 >16 kHz, and beyond 50% perforation, DPOAE levels were usually reduced to the noise floor. The fact that DPOAEs were reduced with increasing size of TM perforation also demonstrated that these high-primary-level induced DPOAEs were from the cochlea, rather than from our recording system.

Reductions in DPOAEs due to TM perforation were similar across animals, which were size-and frequency-dependent (Fig. 2A). These outcomes were categorized into two groups of results and are illustrated by comparison to the normal TM condition in individual and averaged responses (Fig. 2B & D). With smaller TM perforations of up to ~10% (<1/8 of the pars tensa), the subsequent reductions in DPOAE levels were less than 20 dB and appeared to be greater at frequencies around 10–20 kHz in average. Further enlargement of the perforation caused a dramatic frequency-dependent reduction in DPOAEs, which displayed a low-pass filter shape exhibiting wiggles at frequencies below 10 kHz, and quick and dramatic reductions at higher frequencies. For example, compared to the averaged intact measurement, at 25% perforation, there was a 16 dB loss at 3 kHz, 19 dB loss at 5 kHz, and 27 dB loss at 16 kHz. With 50% perforation, the reduction also showed this frequency dependent low-pass filter shape with much greater loss occurring at the higher frequencies, as there was a 23 dB loss at 3 kHz, 26 dB loss at 5 kHz, and 38 dB loss at 16 kHz compared to the normal condition. By 25–50% perforation, the majority of DPOAE responses across animals were in the noise floor at frequencies above 20 kHz, thus those data points were omitted in the figure.

The size-and frequency-dependent DPOAE reduction patterns due to TM perforation could be explained by the directly measured reduction in ME transmission in the form of MEPG, defined as $|P_{SV}/P_{TM}|$ at the primary frequencies of either f_1 or f_2. Variation of ME transmission is illustrated here as the variation in the MEPG compared to that of the TM normal intact condition from the same animal (Fig. 2C) and averaged across animals (Fig. 2E). The MEPG was ~20–30 dB and was almost flat across frequency under normal conditions in gerbils [Figs. 4D & G and Dong et al. (2006)]. Interestingly, TM perforation induced reductions in MEPG were also size-and frequency-dependent, which could be separated into two categories. With a perforation up to ~10%, reductions in the MEPG increased with increasing the size of the TM perforation and were less frequency-dependent in that MEPG decreased up to ~10 dB with greater reductions at frequencies below ~4–5

kHz. Results were similar to observations described in previous studies, [e.g., (Anthony et al., 1972; Bhusal et al., 2006; Pannu et al., 2011; Voss et al., 2001a)]. Increasing the size of TM perforation appeared to lead more reduction at high frequencies. When the perforation size was greater than ~25%, MEPG showed dramatic reductions that were more frequency-dependent. These reductions appeared to represent a low-pass filter pattern that was relatively flat at frequencies below 10 kHz, quickly sloped down with maximum reductions at ~28 kHz, i.e., more than 40 dB when 100% pars tensa was removed, and then leveled off at frequencies above 35 kHz. Reductions in the MEPG appeared to be the summation of major reductions in the effective drive to the umbo and relatively smaller reductions in the motion along the ossicular chain (Stomackin et al., 2018).

A Student's paired t-test of the MEPG and DPOAEs variation at each perforation condition comparing to the intact TM conditions was performed in three separate frequency bins as described above in Methods, i.e., <10 kHz, 10–30 kHz, and >30 kHz for MEPG, <10 kHz, 10–20 kHz, and >20 kHz for DPOAEs, respectively. The changes in both MEPG and DPOAEs at all perforation conditions had p-values <0.01, demonstrating such changes are statistically significant.

To briefly summarize, reductions in DPOAE levels under conditions of mechanically-induced TM perforations were size-and frequency-dependent. These reductions included ME transmission losses both in the forward and reverse direction, and while the losses in the reverse transmission were greater than the reductions in MEPG, they had a similar frequency dependent pattern that could be separated into two categories: 1) when the TM was perforated up to ~10% (<1/8 of the pars tensa), reductions in DPOAE levels were less frequency-dependent, ~ flat across frequencies with more reduction at low frequencies, and 2) when TM perforations were further enlarged, reductions in the DPOAE levels were like a low-pass filter shape, with less reductions at frequencies below 10 kHz and more dramatic reductions at higher frequencies that then leveled off.

3.2 DPOAEs and ME-sound transmission post-perforation under spontaneously-healed conditions

Characteristics of TM structure and functional restoration during the post-perforation spontaneous healing time course are illustrated by images of the TM, ABR thresholds, and DPOAEs measured at key time points, which were followed by directly measured MEPGs at post-perforation week 5 (Figs. 3 & 4). Fig. 3A describes a clear and transparent normal TM. Following a 50% perforation of the pars tensa (Fig. 3B), the healing of the TM occurred quickly and appeared to seal up from the edge to the center, which is consistent with observations in the literature (Johnson et al., 1990; Rahman et al., 2007). By 1-week post-perforation the majority of the perforation was sealed up with only a tiny hole equating ~ 5–8% remaining (Fig. 3C). By 2- week post-perforation, the TM perforation had completely closed (Fig. 3D), however, it had not yet recovered to its normal appearance and appeared to be thicker compared to its intact stage. The recovery of the TM continued as time passed and images of the TM at 3-week (Fig. 3E) were similar to those of 2-week post-perforation apart from some lessening of the opaque scar tissue seen in the healed area. At 4-week post-perforation, the TM's transparency started to look more like the normal condition (Fig. 3F),

however many portions of the TM still had visibly thickened areas. This thickness progression was consistent with reports of the healed TM being considerably thickened at 4-week post-perforation, and even staying noticeably thicker than normal up to 6 months post-perforation (Rahman et al., 2007).

Even though the TM perforation appeared to be significantly healed structurally by 2-week post-perforation, the functional restoration as evaluated by ABR thresholds and DPOAEs over the healing process continued to progress throughout the post-perforation interval. Before the TM perforation, normal ABR thresholds of gerbils were around 10 dB SPL at frequencies between 8–22 kHz, and higher at lower and higher frequencies (the gray line in Fig. 4A), which is consistent with published gerbil ABR thresholds and behavioral audiograms (Boettcher et al., 1993; Ryan, 1976). A 50% TM perforation of pars tensa (Figs. 1C & 2B) led to an elevation of thresholds in a frequency-dependent manner which was more dramatic at 30 dB or more for low-(<2 kHz) and high-frequency regions (>20 kHz), but was 15–20 dB at frequencies between 5–22 kHz (the black dotted lines in Figs. 4A & E). At 1-week post-perforation, ABR thresholds started to recover at essentially all test frequencies, though the recovery in the mid frequencies was small (blue lines in Figs. 4A & E). By 2-week post-perforation, ABR thresholds continued recovering across frequency leaving a difference of 10–15 dB at frequencies below 20 kHz compared to normal TM condition (green lines in Figs. 4A & E). At the higher frequencies, up to ~25 dB difference still existed. By 3-and 4-week post-perforation, ABR thresholds were basically back to normal levels at the majority of frequencies between 2–16 kHz (red lines in Figs. 4A & E). However, elevations of ABR thresholds were still apparent at both lower and higher frequencies, with more loss remaining in the high frequencies (responses of 3-week post perforation were similar to those of 4-week post-perforation and thus not shown). After the 4-week measurements, ABR thresholds appeared to be stabilized at these levels, even up to 8-week post-perforation (notshown).

Restoration of the $2f_1-f_2$ DPOAEs over the time course of healing ((Figs. 4B, C & F) was similar to that of ABR thresholds but was not exactly the same, especially at 1-week post-perforation. With 75 dB SPL equilevel stimulation (f_2/f_1=1.25), DPOAEs were robust between 40–50 dB SPL across test frequencies (gray line in Fig. 4B). The level/pattern differences in DPOAEs as compared to Fig. 2 (see methods section) were probably due to using different data acquisition systems, different microphone and speakers using different sound calibration methods (i.e., *in vivo* at the TM versus on a stimulated gerbil ear canal), and different sound configurations (open-versus closed-sound configuration and with or without the pinna). Post 50% perforation of pars tensa, DPOAEs significantly decreased at all test frequencies, with a greater reduction at frequencies below 10 kHz and above 25 kHz (black dotted line in Figs. 4B, C & F). By 1-week post-perforation, DPOAEs began to recover, especially at f2 frequencies up to 10 kHz (blue lines). An interesting pattern to note is that at the 1-week post-perforation, the low to mid frequencies started to recover while the high-frequency DPOAEs decreased further to the noise floor. The restoration of DPOAEs at frequencies below 20 kHz continued over the recovery time course up to 2-week post-perforation, with a decrease of only 20–30 dB remaining, however, there was little improvement at frequencies above 20 kHz (green lines). On average, by 4-week post-perforation, the reductions in DPOAE levels were still about 10–20 dB lower at frequencies

below 20 kHz compared to the normal condition, even though ABR thresholds were almost back to normal values. At higher frequencies, DPOAE magnitudes were only slightly recovered as they were still ~40 dB lower than those measured under normal TM conditions.

Since MEPG measures acted as a direct representation of ME transmission in the forward direction, they helped to understand the reductions observed for ABR thresholds and DPOAE levels post-perforation. Compared to normal TM conditions in an individual animal (Fig. 4D) and averaged results across animals (Fig. 4G), the MEPG appeared to nearly fully recover up to 8 kHz. However, between ~10 and 25 kHz, the recovered MEPG deviated by 5–10 dB, and significant differences of up to 30 – 40 dB were present at the higher frequencies.

The Student's paired *t*-test of recovered ABR thresholds, DPOAEs at key time points and the MEPG at 5-week post-perforation comparing to normal TM conditions was performed in three frequency bins as described above in the Methods, and the change caused over the recovery time course had a value of $p<0.01$ in most of the three ranges confirming their statistical significance, except at 4-/or 5-week at frequencies below 10 kHz.

For the MEPG, the spontaneously-healed ears showed a clear pattern of near recovery up to 8 kHz, with a sloping decrease in the mid to high frequencies then leveled off. Because of this, we averaged and analyzed the means across frequency within two different frequency ranges: ≤8 kHz (0.5–8 kHz) and ≥8 kHz (8.5–50 kHz). The change between normal and recovered ears up to 8 kHz frequency was not statistically significant, with $p>0.05$. In fact, in most cases, there was little to no change at all between the normal and recovered ears in this frequency bin. For example, both the normal and recovered data had a value of 19.7 dB at 1.5 kHz, and at 7 kHz, the difference between the two was <1 dB. However, >8 kHz, a sloping decrease was seen, and this difference had a p-value <0.01, indicating that the change was statistically significant. Since the healed MEPG had both shallower and steeper slopes within this range, we broke that frequency bin down even farther and analyzed the differences between 8.5–30 kHz and 30–50 kHz separately. Those regions had $p<0.01$ indicating statistically significant differences for both ranges.

4. Discussion

To address the usefulness of DPOAEs under pathological TM conditions, DPOAEs were measured *in vivo* in gerbils under two contrasting TM conditions. One experimental condition involved varying the size of a mechanically-induced TM perforation progressing systematically from miniscule (<3%) to up to 100% removal of the pars tensa, while the other experimental state investigated the spontaneous healing of a 50% TM perforation over a 4-week time course. To further our understanding of the reductions in DPOAE levels under these conditions, direct measures of ME transmission in the form of MEPG were obtained.

Mechanically-induced TM perforations have been shown to be similar to TM perforations caused by intense acoustic blasts (Cho et al., 2013), but the advantage of our study was that we could study these effects in isolation, i.e., without the confounding effects of multiple sites of damage to the ossicular chain, or a resulting sensorineural hearing loss. Similar to

the published studies on TM perforations in the guinea pig and mouse (LeBourgeois et al., 2000; Qin et al., 2010; Ueda et al., 1998), 2-tone evoked DPOAEs were measurable with up to a 50% of TM perforation of the pars tensa and showed frequency-dependent systematic decreases in magnitude with increases in the size of TM perforations (Figs. 2A, B & D). With smaller TM perforations of up to ~10%, reductions in DPOAE levels were less frequency-dependent and appeared to be relatively flat across test frequencies with more reduction at low frequencies. Further enlargement of the perforation caused a dramatic frequency-dependent reduction in DPOAEs, like a low-pass filter shape, with less loss at frequencies below 10 kHz and steep reduction at frequencies above. The reduction pattern across frequencies of DPOAEs was similar to that of the reduction in ME forward transmission as described by the MEPG in the same frequency region (Figs. 2C & E), and appeared to be much greater than reductions seen in the MEPG. Thus, the reduction in DPOAEs included lower primary f1 and f2 levels, because of less efficient ME transmission in the forward direction and a reduced distortion-product component traveling back through the ME to the ear canal. Prior literature noted that gerbil ME forward and reverse transmissions are similar when plotted versus frequency, but there is more pressure loss in the reverse direction than the pressure gain in the forward direction (Dong et al., 2006; Dong et al., 2012). The effects of TM perforation on MEPG in the forward direction were summarized in Fig. 2E, which showed a size-and frequency-dependent pattern that was primarily due to the less efficient drive of the umbo and reduction of the transmission through the ossicular chain under TM-perforation conditions (Stomackin et al., 2018). In addition, the influence of TM perforation on ME transmission in the reverse direction appeared to be similar to those in the forward direction, with a detailed description of the results being prepared in a follow-up report as well. DPOAEs have also been used in studies of blast-induced hearing loss mechanisms using mice and chinchillas (Cho et al., 2013; Hickman et al., 2018). The middle and inner ear appeared to be the most vulnerable structures in the body to blast-wave exposure and more than 70% showed TM perforations. In these studies, DPOAE threshold shifts were normally found to be greater than those evaluated using ABR or compound action potential responses in TM perforated ears, which was explained by the reduction of the ME transmission. In addition, TM perforation was suggested to be a protective mechanism during blast or noise exposure because less inner ear injuries were found in the TM perforated cases. However, since these studies were using ears with mixed ME and inner ear injuries, the effects of blast waves vs. TM perforation to the middle and inner ear could not be differentiated clearly. On the contrary, the uniqueness of the current study of the effects of TM perforation on DPOAEs can be described in several ways including that the DPOAEs were measured over a broad frequency region, TM perforation was systematically enlarged in a series of mechanically-induced perforations, and ME transmission was directly measured in the form of the MEPG. Thus, our results contributed to forming clinical guidelines for using DPOAEs as a diagnostic tool following TM perforations.

Our results also suggest that DPOAEs are measurable after a 50% perforation during the spontaneous TM healing process and recover in a similar manner as those characterized by the recovery of ABR thresholds except at 1-week post-perforation with further reductions at high frequencies (Figs. 3 & 4). After 4-week post-perforation, both ABR thresholds and

DPOAEs appeared to be almost back to normal between 2–10 kHz, however high-frequency ABR thresholds and DPOAEs were still not back to their normal values, which correlated with the decreased MEPG at these frequencies. Our results were consistent with hearing recovery results of the spontaneous closure of TM perforations in patients who experienced blast injuries during the Boston Marathon on April 15, 2013 (Remenschneider et al., 2014). The air conduction thresholds of these patients recovered within 10 dB HL (hearing level) at frequencies below 2 kHz then showed a sloping downward pattern at higher frequencies.

Furthermore, DPOAEs showed more reductions compared to that of ABR thresholds, in general, thus confirming the fact that DPOAEs are influenced by ME-transmission in both the forward and reverse directions. This outcome supports the claim that DPOAEs are more sensitive to such pathological TM conditions than ABRs. The considerable effects of TM perforations on ME transmission in the reverse direction were confirmed by the observation that significant reductions in DPOAEs up to 20 kHz of about 10–20 dB after 4 weeks of healing were still present, while ABR thresholds were almost back to normal. However, at frequencies above 20 kHz, both DPOAEs and ABRs still showed significant deviations from the normal condition.

There were some differences in the level and pattern of DPOAEs when comparing the mechanically-induced TM perforation results to the spontaneously-healed TM results that were due to differences in the experimental system and conditions, which were described in detail in section 2 of Materials and methods. The mechanically-induced experiment was performed in animals that had their pinna and ear canal removed and bullae widely opened. The sound delivered for this experiment was also in an open-field configuration due to the necessity of making a small hole superior to the ear canal opening to access the TM to create perforations. This directly contrasts with the set up used for the spontaneously-healed experiment, as in that experiment, the sound was delivered in a closed-field configuration to gerbils that had no surgery performed on them, so the pinna and ear canal were left intact. The setting and results should be more comparable to clinically measured DPOAEs.

It has been reported that spontaneously-healed TMs are thicker and denser than normal and thus contribute to the resulting elevated hearing thresholds observed in patients (Cho et al., 2013; Garth, 1994). It has been found that after healing, TMs display a thickened membrane not only over the healed-perforation locus but also on areas adjacent to the perforation (Rahman et al., 2007; Rahman et al., 2005). In addition, when the healing process begins, it is the epidermis closest to the perforation that thickens and advances to cover the perforation. However, the leading edge of this healing membrane is usually unevenly shaped, which ultimately results in a highly variable thickness of the restored tissue (Johnson et al., 1990). Our preliminary thickness data confirms this, as we have seen that the healed perforated region was more than 2x thicker than a normal TM at week-5 post-perforation and that these thicker regions extended past the perforation area to parts of the superior portion of the pars tensa (normal vs. healed thickness measurements are currently being developed into a separate manuscript). It is likely that the increased thickness of the spontaneously-healed TMs contributed to the abnormalities of DPOAEs, ABRs, and MEPG post-4-week recovery that we observed.

Our data demonstrated the potential clinical application of DPOAEs under these TM pathological conditions as a noninvasive tool with frequency dependent variation patterns that compensate for conventional methods, as they frequently fail to fully identify this common ME problem (Lerut et al., 2012; Margolis et al., 1987; Shanks, 1984). For example, tympanometry often produces the same pattern for widely different ME pathologies, or inversely, the same ME pathology may produce different tympanometry readings (Shanks, 1984). The frequency-dependent pattern seen in DPOAEs allowed us to differentiate losses due to a CHL from patterns of sensorineural hearing loss. Our results demonstrated that DPOAEs were sensitive to ME function, and showed greater reductions when comparing the directly measured ME transmission in the form of MEPG or ABR thresholds. This is because the DPOAE reduction was a summation of ME transmission losses both in the forward and reverse directions. On the other hand, frequency-dependent loss patterns of DPOAEs in cases of sensorineural hearing loss were comparable or smaller than evaluated ABR thresholds or compound action potential thresholds because of their widely distributed generation nature in the cochlea [i.e., (Dong, 2017; Dong et al., 2010; Harding et al., 2004; Harding et al., 2002; Martin et al., 2010; Martin et al., 2009)]. Therefore, our results showed the power that DPOAEs could be used as a fast and accurate diagnostic tool in ME disorders.

5. Conclusion

In summary, the data from gerbils presented here demonstrated the ability to use DPOAEs to monitor ME function and highlighted their capability to compensate for current conventional clinical methods, which are lacking in their ability to accurately describe hearing patterns under pathological TM conditions. DPOAEs are a quick and precise diagnostic tool, and are especially useful as the reduced DPOAE-level patterns across test frequencies produced by a CHL can be separated from those resulting from a sensorineural hearing impairment. Additionally, DPOAEs reflect not only the forward transmission of the primary-tones through the ME, but also the reverse transmission of DPOAEs that are generated in the cochlea back to the ear canal (Shera et al., 1999). The effects of TM perforation on DPOAEs can be categorized into two groups. First, with a smaller-sized TM perforation, i.e., up to 10%, reductions in DPOAE levels were almost flat across test frequency. And second, larger perforations with a size of more than 10% led to a low-pass filter reduction pattern. These patterns were consistent with the losses in ME transmission in the forward and reverse directions, as the loss in the reverse direction was almost twice that in the forward direction. We also found that post-perforation, DPOAEs only partially recovered as the TM spontaneously-healed and were more sensitive than evaluations by ABR thresholds. In addition, our data also suggested that the CHLs observed in patients with healed TMs, especially at the higher frequencies, were due to a non-perfect restoration of the ME-transmission system. Thus, the current study advances the otological field’s understanding of the role of the TM on ME transmission under such pathological conditions.

Acknowledgments

The authors would like to thank Mike Xing for helping to confirm the perforation sizes using available intact ears to mimic the experimental conditions. This study, conducted at facilities provided by the US Department of Veterans Affairs, was supported by funding from the Department of Veterans Affairs (Merit Award C2296-R to W Dong) and

the National Institutes of Health (NIDCD DC011506 to W Dong), along with funding from the Department of Otolaryngology, Head and Neck Surgery at Loma Linda University Health. These contents do not represent the views of the US Department of Veterans Affairs nor the United States Government.

Glossary

ABR	auditory brainstem response
CHL	conductive hearing loss
dB	decibel
DP-gram	DPOAE levels as a function of f_2 frequencies
DPOAE	distortion product otoacoustic emission
FFT	fast Fourier transform
ME	middle ear
MEPG	middle ear pressure gain
OAE	otoacoustic emission
P_{TM}	TM pressure near the umbo
P_{SV}	pressure in scala vestibuli next to the stapes
SD	standard deviation
SPL	sound pressure level
SV	scala vestibuli
TM	tympanic-membrane

References

Allen JB, Fahey PF 1992 Using acoustic distortion products to measure the cochlear amplifier gain on the basilar membrane. The Journal of the Acoustical Society of America 92, 178–88. [PubMed: 1512322]

Anthony WP, Harrison CW 1972 Tympanic membrane perforation. Effect on audiogram. Arch Otolaryngol 95, 506–10. [PubMed: 4666421]

Bhusal CL, Guragain RP, Shrivastav RP 2006 Size of typmanic membrane perforation and hearing loss. JNMA; journal of the Nepal Medical Association 45, 167–72. [PubMed: 17160091]

Boettcher FA, Mills JH, Norton BL 1993 Age-related changes in auditory evoked potentials of gerbils. I. Response amplitudes. Hearing research 71, 137–45. [PubMed: 8113132]

Buytaert JA, Salih WH, Dierick M, Jacobs P, Dirckx JJ 2011 Realistic 3D computer model of the gerbil middle ear, featuring accurate morphology of bone and soft tissue structures. Journal of the Association for Research in Otolaryngology 12, 681–96. [PubMed: 21751073]

Cho SI, Gao SS, Xia A, Wang R, Salles FT, Raphael PD, Abaya H, Wachtel J, Baek J, Jacobs D, Rasband MN, Oghalai JS 2013 Mechanisms of hearing loss after blast injury to the ear. PLoS One 8, e67618. [PubMed: 23840874]

Cohen YE, Bacon CK, Saunders JC 1992 Middle ear development. III: Morphometric changes in the conducting apparatus of the Mongolian gerbil. Hearing research 62, 187–93. [PubMed: 1429261]

Dalhoff E, Turcanu D, Gummer AW 2011 Forward and reverse transfer functions of the middle ear based on pressure and velocity DPOAEs with implications for differential hearing diagnosis. Hearing research 280, 86–99. [PubMed: 21624450]

de Boer E, Nuttall AL, Hu N, Zou Y, Zheng J 2005 The Allen-Fahey experiment extended. Journal of the Acoustical Society of America 117, 1260–1266. [PubMed: 15807015]

Dong W 2017 Simultaneous Intracochlear Pressure Measurements from Two Cochlear Locations: Propagation of Distortion Products in Gerbil. Journal of the Association for Research in Otolaryngology : JARO 18, 209–225. [PubMed: 27909837]

Dong W, Olson ES 2006 Middle ear forward and reverse transmission in gerbil. Journal of neurophysiology 95, 2951–61. [PubMed: 16481455]

Dong W, Olson ES 2008 Supporting evidence for reverse cochlear traveling waves. The Journal of the Acoustical Society of America 123, 222–40. [PubMed: 18177153]

Dong W, Olson ES 2010 Local cochlear damage reduces local nonlinearity and decreases generator-type cochlear emissions while increasing reflector-type emissions. The Journal of the Acoustical Society of America 127, 1422–31. [PubMed: 20329842]

Dong W, Olson ES 2013 Detection of cochlear amplification and its activation. Biophysical journal 105, 1067–78. [PubMed: 23972858]

Dong W, Decraemer WF, Olson ES 2012 Reverse transmission along the ossicular chain in gerbil. Journal of the Association for Research in Otolaryngology : JARO 13, 447–59. [PubMed: 22466074]

Dong W, Tian Y, Gao X, Jung TT 2017 Middle-Ear Sound Transmission Under Normal, Damaged, Repaired, and Reconstructed Conditions. Otol Neurotol 38, 577–584. [PubMed: 28079680]

Garth RJ 1994 Blast injury of the auditory system: a review of the mechanisms and pathology. The Journal of laryngology and otology 108, 925–9. [PubMed: 7829942]

Harding GW, Bohne BA 2004 Temporary DPOAE level shifts, ABR threshold shifts and histopathological damage following below-critical-level noise exposures. Hearing research 196, 94–108. [PubMed: 15464306]

Harding GW, Bohne BA, Ahmad M 2002 DPOAE level shifts and ABR threshold shifts compared to detailed analysis of histopathological damage from noise. Hearing research 174, 158–71. [PubMed: 12433407]

Hickman TT, Smalt C, Bobrow J, Quatieri T, Liberman MC 2018 Blast-induced cochlear synaptopathy in chinchillas. Sci Rep 8, 10740. [PubMed: 30013117]

Johnson AP, Smallman LA, Kent SE 1990 The mechanism of healing of tympanic membrane perforations. A two-dimensional histological study in guinea pigs. Acta oto-laryngologica 109, 406–15. [PubMed: 2360447]

Keefe DH 2002 Spectral shapes of forward and reverse transfer functions between ear canal and cochlea estimated using DPOAE input/output functions. The Journal of the Acoustical Society of America 111, 249–60. [PubMed: 11831799]

Kemp DT 1978 Stimulated acoustic emissions from within the human auditory system. The Journal of the Acoustical Society of America 64, 1386–91. [PubMed: 744838]

LeBourgeois HW 3rd, Anand VK, McAuley JR, Dickman JD, Malphurs O Jr. 2000 Effect of tympanic perforations on the detection of distortion-product otoacoustic emissions. Ear Nose Throat J 79, 610–2, [PubMed: 10969471]

Lerut B, Pfammatter A, Moons J, Linder T 2012 Functional correlations of tympanic membrane perforation size. Otol Neurotol 33, 379–86. [PubMed: 22334155]

Lonsbury-Martin BL, Martin GK 1990 The clinical utility of distortion-product otoacoustic emissions. Ear and hearing 11, 144–54. [PubMed: 2187725]

Magnan P, Avan P, Dancer A, Smurzynski J, Probst R 1997 Reverse middle-ear transfer function in the guinea pig measured with cubic difference tones. Hearing research 107, 41–5. [PubMed: 9165345]

Margolis RH, Heller JW 1987 Screening tympanometry: criteria for medical referral. Audiology 26, 197–208. [PubMed: 3632475]

Martin GK, Stagner BB, Lonsbury-Martin BL 2010 Evidence for basal distortion-product otoacoustic emission components. The Journal of the Acoustical Society of America 127, 2955–72. [PubMed: 21117746]

Martin GK, Stagner BB, Fahey PF, Lonsbury-Martin BL 2009 Steep and shallow phase gradient distortion product otoacoustic emissions arising basal to the primary tones. The Journal of the Acoustical Society of America 125, EL85–92. [PubMed: 19275280]

Martin GK, Stagner BB, Chung YS, Lonsbury-Martin BL 2011 Characterizing distortion-product otoacoustic emission components across four species. The Journal of the Acoustical Society of America 129, 3090–103. [PubMed: 21568412]

Mason MJ 2016 Structure and function of the mammalian middle ear. II: Inferring function from structure. Journal of Anatomy 228, 300–12. [PubMed: 26100915]

McArdle FE, Tonndorf J 1968 Perforations of the tympanic membrane and their effects upon middle-ear transmission. Arch Klin Exp Ohren Nasen Kehlkopfheilkd 192, 145–62. [PubMed: 5719315]

Mehta RP, Rosowski JJ, Voss SE, O'Neil E, Merchant SN 2006 Determinants of hearing loss in perforations of the tympanic membrane. Otol Neurotol 27, 136–43. [PubMed: 16436981]

Merchant SN, Rosowski JJ, McKenna MJ 2003a Tympanoplasty. Operative Techiniques in Otolaryngology-Head and Neck Surgery 14, 224–236.

Merchant SN, McKenna MJ, Mehta RP, Ravicz ME, Rosowski JJ 2003b Middle ear mechanics of Type III tympanoplasty (stapes columella): II. Clinical studies. Otol Neurotol 24, 186–94. [PubMed: 12621330]

Naghibolhosseini M, Long GR 2017 Estimation of Round-Trip Outer-Middle Ear Gain Using DPOAEs. Journal of the Association for Research in Otolaryngology 18, 121–138. [PubMed: 27796594]

Olson ES 1998 Observing middle and inner ear mechanics with novel intracochlear pressure sensors. The Journal of the Acoustical Society of America 103, 3445–63. [PubMed: 9637031]

Pannu KK, Chadha S, Kumar D, Preeti. 2011 Evaluation of hearing loss in tympanic membrane perforation. Indian journal of otolaryngology and head and neck surgery : official publication of the Association of Otolaryngologists of India 63, 208–13.

Park H, Hong SN, Kim HS, Han JJ, Chung J, Suh MW, Oh SH, Chang SO, Lee JH 2015 Determinants of conductive hearing loss in tympanic membrane perforation. Clinical and experimental otorhinolaryngology 8, 92–6. [PubMed: 26045905]

Probst R, Lonsbury-Martin BL, Martin GK 1991 A review of otoacoustic emissions. The Journal of the Acoustical Society of America 89, 2027–67. [PubMed: 1860995]

Puria S 2003 Measurements of human middle ear forward and reverse acoustics: implications for otoacoustic emissions. The Journal of the Acoustical Society of America 113, 2773–89. [PubMed: 12765395]

Puria S, Fay RR, Popper A 2013 The Middle Ear, Springer Handbook of Auditory Research, Vol. 46, 1 ed. Springer-Verlag New York pp. 1–308.

Qin Z, Wood M, Rosowski JJ 2010 Measurement of conductive hearing loss in mice. Hearing research 263, 93–103. [PubMed: 19835942]

Rahman A, Hultcrantz M, Dirckx J, von Unge M 2007 Structural and functional properties of the healed tympanic membrane: a long-term follow-up after laser myringotomy. Otol Neurotol 28, 685–91. [PubMed: 17429337]

Rahman A, Hultcrantz M, Dirckx J, Margolin G, von Unge M 2005 Fresh tympanic membrane perforations heal without significant loss of strength. Otol Neurotol 26, 1100–6. [PubMed: 16272923]

Ravicz ME, Rosowski JJ, Voigt HF 1992 Sound-power collection by the auditory periphery of the Mongolian gerbil Meriones unguiculatus. I: Middle-ear input impedance. Journal of the Acoustical Society of America 92, 157–77. [PubMed: 1512321]

Remenschneider AK, Lookabaugh S, Aliphas A, Brodsky JR, Devaiah AK, Dagher W, Grundfast KM, Heman-Ackah SE, Rubin S, Sillman J, Tsai AC, Vecchiotti M, Kujawa SG, Lee DJ, Quesnel AM 2014 Otologic outcomes after blast injury: the Boston Marathon experience. Otol Neurotol 35, 1825–34. [PubMed: 25393974]

Ryan A 1976 Hearing sensitivity of the mongolian gerbil, Meriones unguiculatis. The Journal of the Acoustical Society of America 59, 1222–6. [PubMed: 956517]

Shanks JE 1984 Tympanometry. Ear and hearing 5, 268–80. [PubMed: 6542036]

Shera CA 2004 Mechanisms of mammalian otoacoustic emission and their implications for the clinical utility of otoacoustic emissions. Ear and hearing 25, 86–97. [PubMed: 15064654]

Shera CA, Guinan JJ Jr. 1999 Evoked otoacoustic emissions arise by two fundamentally different mechanisms: a taxonomy for mammalian OAEs. The Journal of the Acoustical Society of America 105, 782–98. [PubMed: 9972564]

Shera CA, Guinan JJ Jr. 2007 Cochlear traveling-wave amplification, suppression, and beamforming probed using noninvasive calibration of intracochlear distortion sources. The Journal of the Acoustical Society of America 121, 1003–16. [PubMed: 17348523]

Stomackin G, Kidd S, Jung TT, Martin GK, Dong W 2018 Effects of tympanic membrane perforation on middle ear transmission in gerbil. Hearing research 373, 48–58. [PubMed: 30583199]

Teoh SW, Flandermeyer DT, Rosowski JJ 1997 Effects of pars flaccida on sound conduction in ears of Mongolian gerbil: acoustic and anatomical measurements. Hearing research 106, 39–65. [PubMed: 9112106]

Tlumak A, Kileny P 2001 Parameters that affect the measurement of otoacoustic emissions. Otolaryngol Head Neck Surg, 279–283. [PubMed: 11240991]

Ueda H, Nakata S, Hoshino M 1998 Effects of effusion in the middle ear and perforation of the tympanic membrane on otoacoustic emissions in guinea pigs. Hearing research 122, 41–6. [PubMed: 9714573]

Voss SE, Shera CA 2004 Simultaneous measurement of middle-ear input impedance and forward/reverse transmission in cat. The Journal of the Acoustical Society of America 116, 2187–98. [PubMed: 15532651]

Voss SE, Rosowski JJ, Merchant SN, Peake WT 2000 Acoustic responses of the human middle ear. Hearing research 150, 43–69. [PubMed: 11077192]

Voss SE, Rosowski JJ, Merchant SN, Peake WT 2001a Middle-ear function with tympanic-membrane perforations. II. A simple model. The Journal of the Acoustical Society of America 110, 1445–52. [PubMed: 11572355]

Voss SE, Rosowski JJ, Merchant SN, Peake WT 2001b Middle-ear function with tympanic-membrane perforations. I. Measurements and mechanisms. The Journal of the Acoustical Society of America 110, 1432–44. [PubMed: 11572354]

Voss SE, Rosowski JJ, Merchant SN, Peake WT 2007 Non-ossicular signal transmission in human middle ears: Experimental assessment of the “acoustic route” with perforated tympanic membranes. The Journal of the Acoustical Society of America 122, 2135–53. [PubMed: 17902851]

Zhao F, Wada H, Koike T, Stephens D 2000 The influence of middle ear disorders on otoacoustic emissions. Clin Otolaryngol Allied Sci 25, 3–8. [PubMed: 10764230]

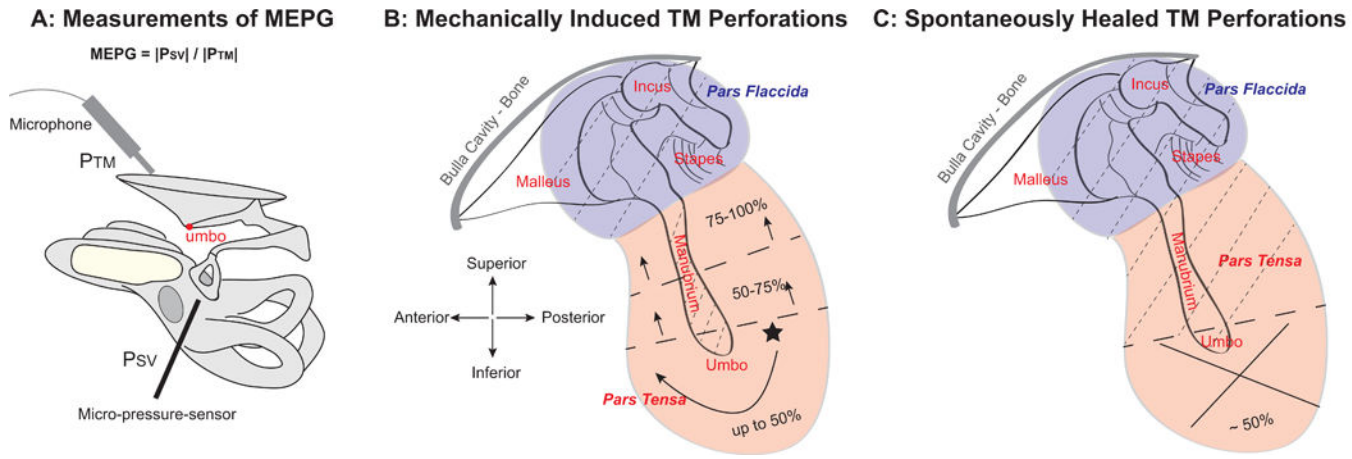

Figure 1. Illustration of quantitative measures of MEPG and TM perforation conditions.

(A) Experimental approach for simultaneous measurements of P_{TM} and P_{SV} using an ultrasound Sokolich probe-tube microphone and a micro-pressure sensor positioned close to the TM and in the SV next to the stapes, respectively. ME pressure gain was defined as MEPG = $|P_{SV}| / |P_{TM}|$. P_{TM}: pressure at the TM; P_{SV}: pressure in the SV next to the stapes.; SV: scala vestibuli. **(B)** Diagram of mechanically induced TM perforations re size and location. The initial perforation was made at a location in the inferior pars tensa (star) using a 200-μm diameter sterilized pin, and was then subsequently enlarged to the desired size, i.e., ~ <1/8 (10%), 1/4 (25%), 1/2 (50%), 3/4 (75%), and 100%, by carefully expanding the edges of the existing perforation clockwise until the pars tensa was completely removed, leaving only the pars flaccida, the TM directly on top of the manubrium, and the ossicular chain intact. **(C)** Diagram of a ~50% TM perforation at the inferior location of the pars tensa, which spontaneously-healed up to 4 weeks. Dashed lines in panels B & C indicate areas of the TM that were left intact.

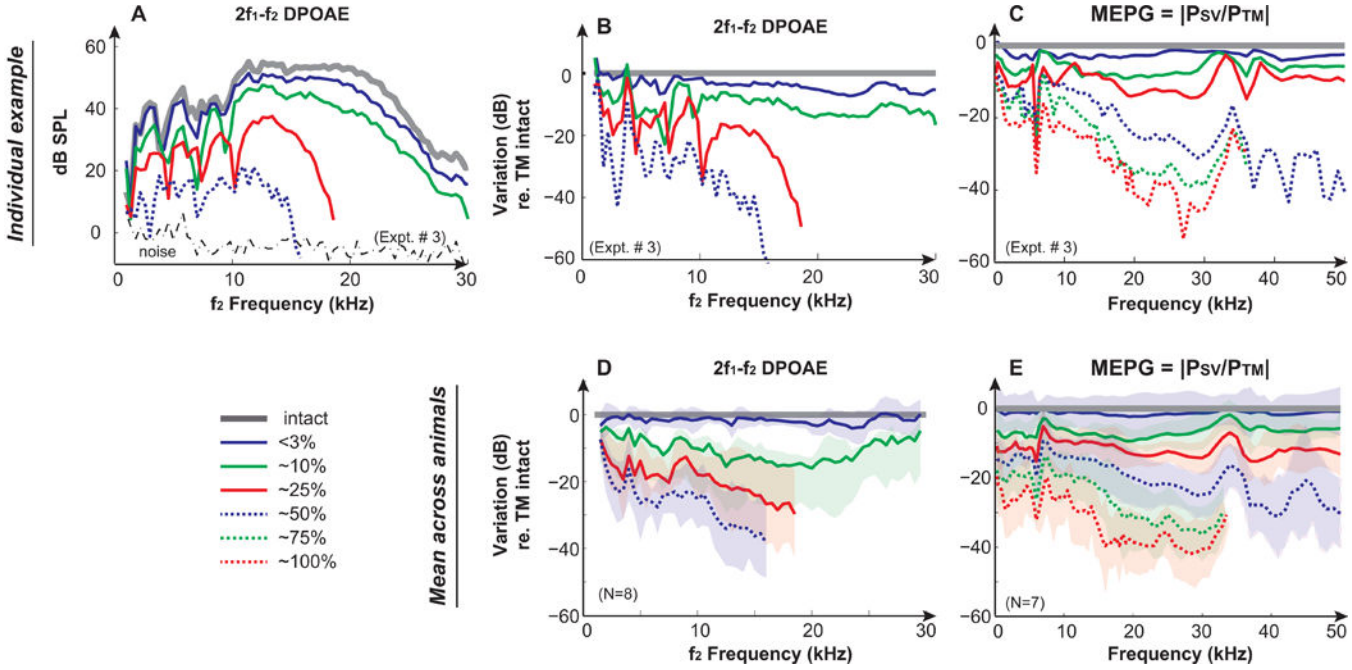

Figure 2. Effects of mechanically induced TM perforations on DPOAEs and MEPG.

Results from a representative animal (Expt. #3) of **(A)** $2f_1-f_2$ DPOAEs under TM intact and perforated conditions. DPOAEs were induced by 2 equilevel ($L_1=L_2$) f_1 and f_2 primary tones at 90 dB SPL with an f_2/f_1 ratio of 1.25; Variations of **(B)** DPOAEs and **(C)** MEPG under TM perforation conditions compared to the intact TM condition in the same animal. Averaged results across animals of variations of **(D)** DPOAEs and **(E)** MEPG under TM perforation conditions compared to the intact TM condition. Gray lines represent the normal intact TM condition. Solid blue, green, and red lines represent <3%, ~10%, and ~25% removal of the pars tensa, respectively. Dashed blue, green, and red lines indicate 50%, 75%, and 100% removal of the pars tensa, respectively. Shaded areas in D & E represent mean ± 1 standard deviation. DPOAEs and MEPG could be measured with TM perforations up to 50% and 100%, respectively. Missing data points were in the noise floor and were removed for clarification.

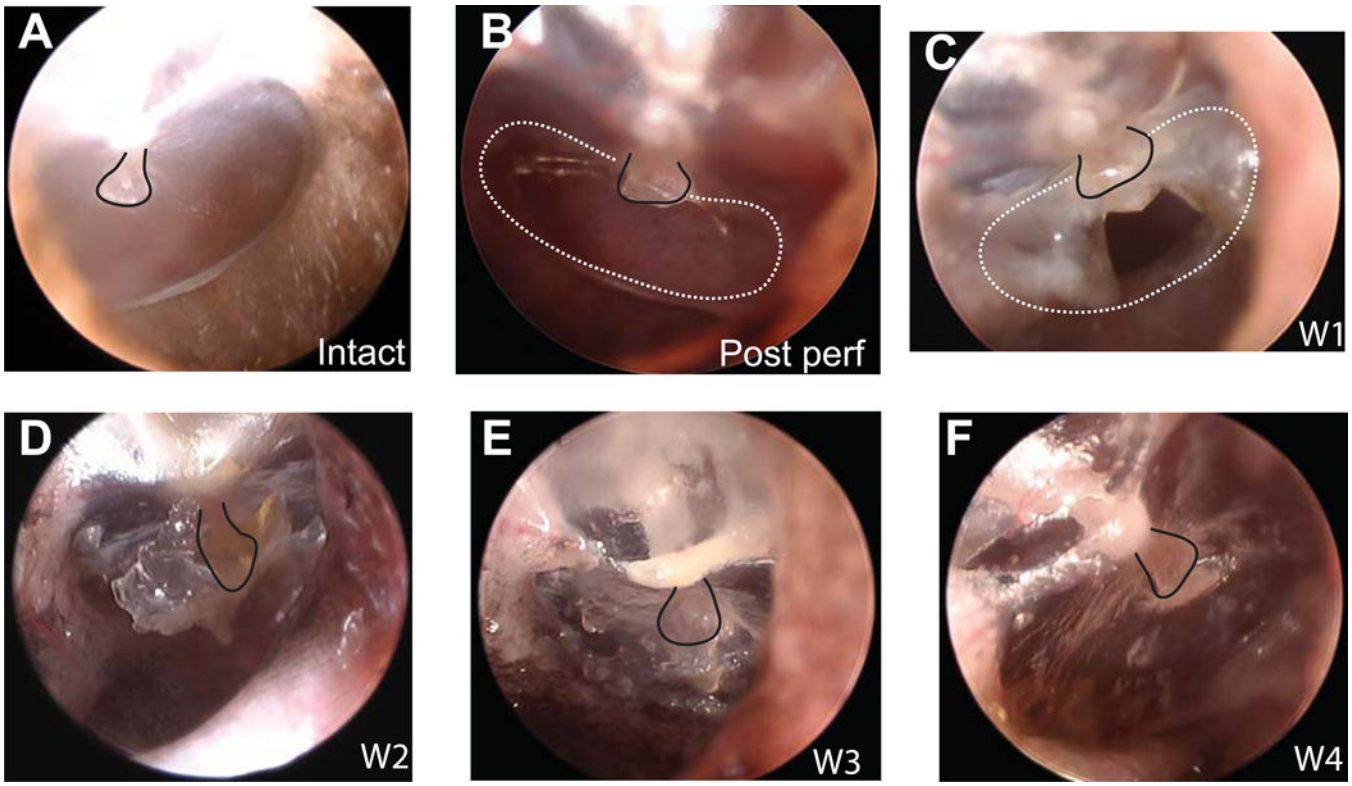

Figure 3. Otoscopic pictures of the TM during the 50% post-perforation spontaneous healing process.

Pictures of the TM under conditions of **(A)** intact, **(B)** post-perforation, **(C)** 1-week, **(D)** 2-week, **(E)** 3-week, and **(F)** 4-week post-perforation, respectively. The presence of some slight wax build-up is seen during the 2-week post measurement in panel D. To help visualization, black solid lines indicate the umbo/manubrium in all panels, and white dashed lines indicate the perforation area in B & C.

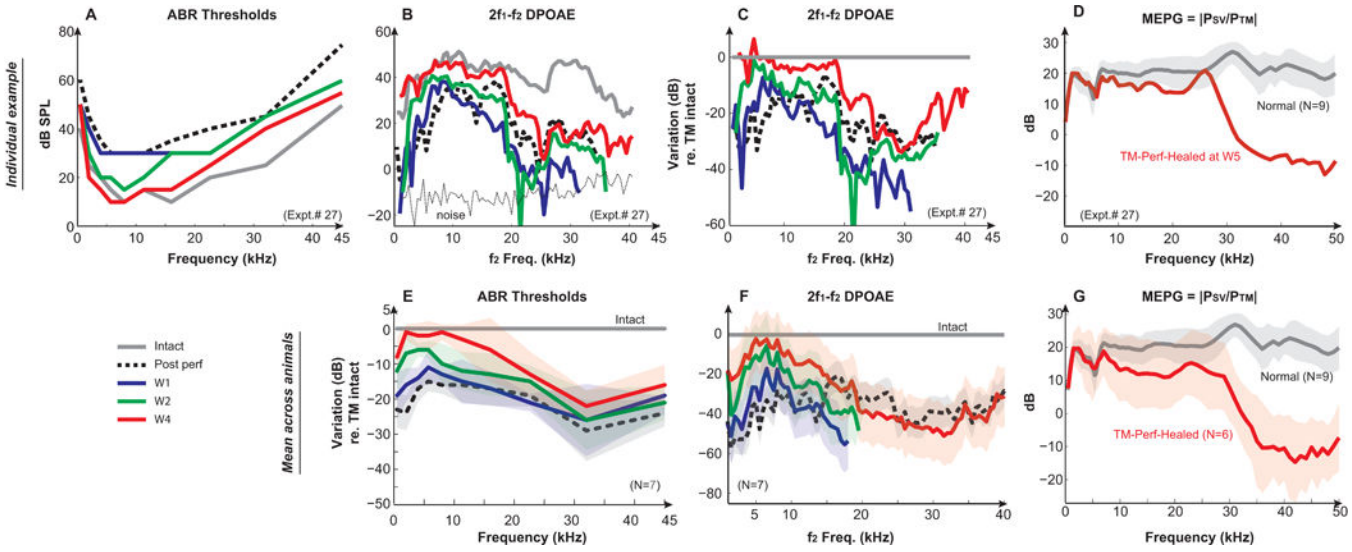

Figure 4. Hearing recoveries during the 50% post-perforation spontaneous healing process.

An individual example of **(A)** ABR thresholds, **(B)** $2f_1-f_2$ DP-grams, and **(C)** the DPOAE variation compared to the TM intact condition over the recovery time period of 4 weeks, as well as the direct measures of **(D)** MEPG after 4-week recovery (from Expt. #27). Averaged variations of **(E)** ABR thresholds and **(F)** DPOAEs compared to that of the TM intact conditions across animals (N=7) at key time points, and **(G)** the averaged MEPG from spontaneously-healed animals measured at 5-week post-perforation conditions (N=6). MEPG under normal conditions (N=9) was plotted as a comparison. DPOAEs were evoked by two-tones of $L_1=L_2=75$ dB SPL with $f_2/f_1=1.25$. Solid gray lines represent the normal/intact condition. Dotted black lines represent the 50% post-perforation condition. Solid blue, green, and red lines represent 1-week, 2-week, and 4-week post perforation, respectively. Results of 3-week were similar to that of 4-week, and thus not shown. Missing data points were in the noise floor and were removed for clarification.